

AD-A197 193

④  
MTC FILE COPY

REPORT DOCUMENTATION PAGE

|   |       |   |                         |
|---|-------|---|-------------------------|
| 1a. REPORT SECURITY CLASSIFICATION<br>Unclassified  |       | 1d. RESTRICTIVE MARKINGS  |                         |
| 2a. SECURITY CLASSIFICATION AUTHORITY   |       | 3. DISTRIBUTION/AVAILABILITY OF REPORT<br>Unlimited   |                         |
| 2b. DECLASSIFICATION/DOWNGRADING SCHEDULE   |       | 3. MONITORING ORGANIZATION REPORT NUMBER(S)   |                         |
| 4. PERFORMING ORGANIZATION REPORT NUMBER(S)<br>Technical Report No. 8   |       | 7a. NAME OF MONITORING ORGANIZATION<br>Office of Naval Research                                 |                         |
| 5a. NAME OF PERFORMING ORGANIZATION<br>The University of Texas at Arlington   |       | 7b. ADDRESS (City, State, and ZIP Code)<br>800 North Quincy Street<br>Arlington, Virginia 22217 |                         |
| 5b. OFFICE SYMBOL (if applicable)   |       | 7c. ADDRESS (City, State, and ZIP Code)<br>1410 Wilson Boulevard<br>Arlington, Virginia 22209   |                         |
| 6a. NAME OF FUNDING/SPONSORING ORGANIZATION<br>Defense Advanced Research Projects Agency  |       | 8a. OFFICE SYMBOL (if applicable)<br>DARPA  |                         |
| 6b. ADDRESS (City, State, and ZIP Code)   |       | 9. PROCUREMENT INSTRUMENT IDENTIFICATION NUMBER<br>N00014-86-K-0769                             |                         |
| 10. SOURCE OF FUNDING NUMBERS   |       | 10. SOURCE OF FUNDING NUMBERS   |                         |
|   |       | PROGRAM ELEMENT NO.   | PROJECT NO.             |
|   |       | TASK NO.  | WORK UNIT ACCESSION NO. |
| 11. TITLE (Include Security Classification)<br>Electronic and Ionic Transport in Polymers   |       |   |                         |
| 12. PERSONAL AUTHOR(S)<br>John R. Reynolds, N.S. Sundaresan, Martin Pomerantz,<br>Sanjiv Basak and Charles K. Baker   |       |   |                         |
| 13a. TYPE OF REPORT<br>Technical  |       | 13b. TIME COVERED<br>FROM _____ TO _____  |                         |
|   |       | 14. DATE OF REPORT (Year, Month, Day)<br>1988 July 12   |                         |
|   |       | 15. PAGE COUNT<br>32  |                         |
| 16. SUPPLEMENTARY NOTATION<br>Journal of Electroanalytical Chemistry, in press  |       |   |                         |
| 17. COSATI CODES  |       | 18. SUBJECT TERMS (Continue on reverse if necessary and identify by block number)               |                         |
| FIELD   | GROUP | SUB-GROUP   |                         |
|   |       | Electroactive polymers, electrochemical charge transport.                                       |                         |
| 19. ABSTRACT (Continue on reverse if necessary and identify by block number)<br>A self-doped copolymer of pyrrole, poly(pyrrole-co[3-(pyrrol-1-yl)propanesulfonate]}, in which the charge compensating counterion is covalently bound to the polymer main chain has been prepared and the charge transport in the polymer during redox switching has been investigated using chronocoulometry and microgravimetry as a function of supporting electrolyte. The results are compared with the behavior of polypyrrole under similar conditions. It is shown that within this new family of materials called self-doped conductive polymers ion mobility is restricted to cationic species and thus the polymer can be viewed as an ion specific membrane. This is in contrast to the case of polypyrrole where a more complex behavior prevails. The charge passed during the chronocoulometric experiment varies as $t^{\alpha}$ where $0.2 < \alpha < 0.9$ and the ion mobility is sensitive to cation size. (A.W.R.) $\alpha$ Alpha |       |   |                         |
| 20. DISTRIBUTION/AVAILABILITY OF ABSTRACT<br><input checked="" type="checkbox"/> UNCLASSIFIED/UNLIMITED <input checked="" type="checkbox"/> SAME AS RPT <input type="checkbox"/> DTIC USERS   |       | 21. ABSTRACT SECURITY CLASSIFICATION<br>Unclassified  |                         |
| 22a. NAME OF RESPONSIBLE INDIVIDUAL<br>Dr. JoAnn Millikan   |       | 22b. TELEPHONE (include Area Code)<br>202-696-1410  |                         |
| 22c. OFFICE SYMBOL  |       | 22d. OFFICE SYMBOL  |                         |

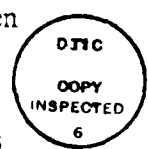
SELF-DOPED CONDUCTING COPOLYMERS: A CHARGE TRANSPORT STUDY OF POLY{PYRROLE-CO-[3-(PYRROL-1-YL)PROPANESULFONATE]}

JOHN R. REYNOLDS\*, N.S. SUNDARESAN, MARTIN POMERANTZ\*, SANJAY BASAK AND CHARLES K. BAKER

Department of Chemistry, The University of Texas at Arlington, Arlington, TX 76019

ABSTRACT

A self-doped copolymer of pyrrole, poly{pyrrole-co-[3-(pyrrol-1-yl)propanesulfonate]}, in which the charge compensating counterion is covalently bound to the polymer main chain has been prepared and the charge transport in the polymer during redox switching has been investigated using chronocoulometry and microgravimetry as a function of supporting electrolyte. The results are compared with the behavior of polypyrrole under similar conditions. It is shown that within this new family of materials called "self-doped conductive polymers" ion mobility is restricted to cationic species and thus the polymer can be viewed as an ion specific membrane. This is in contrast to the case of polypyrrole where a more complex behavior prevails. The charge passed during the chronocoulometric experiment varies as  $\alpha$  where  $0.2 < \alpha < 0.9$  and the ion mobility is sensitive to cation size.



Form with fields: For, &I, ed, tion, tion/, ility Codes, and/or, special. Includes handwritten 'A-1' in a box.

INTRODUCTION

The electrochemical insulator to conductor switching in polypyrrole [1] and similar conductive polymers, such as the polythiophenes [2], is of considerable interest since a complete understanding of the mechanism of charge transport is essential to the design and optimization of such polymer properties. An essential feature of the above process is the transport of counterions into and out of the polymer film as it is cycled between reduced and oxidized states. During these processes the movement of ions into and out of the polymer film limits the rate of charge-transport. In most conductive polymer systems this process is complicated by the fact that the type of the mobile species is controlled by a number of variables. For example, as shown in Scheme I,

reduction of a doped polymer can be accompanied by expulsion of an anion into the electrolyte (Route I) or movement of a cation into the film (Route II) leaving electrolyte in the neutral polymer matrix or a combination of the two. The route followed will be primarily dependent on the nature of the interactions of the ionic species with the charged sites on the polymer backbone. This results in ambiguity in interpreting the charge transport mechanism and in defining transport rates to specific ionic species. Attempts have been made to resolve this problem by in-situ measurement

#### Insert Scheme I

of mass changes in both conductive polypyrrole [3] and polyaniline [4], along with electroactive poly(vinyl ferrocene) [5], during redox switching in a supporting electrolyte. These studies have shown that the identity of the mobile species, anion or cation, is electrolyte dependent. Direct analysis of poly(3-methyl-thiophene) after electrochemical reduction, by XPS and atomic absorption of HNO<sub>3</sub> digested films showed the incorporation of cations from the electrolyte [2b].

Recently, a new family of conductive polymers, termed *self-doped* polymers have been developed [6,7]. In these systems, an electrochemically inert counterion, typically a sulfonate, is covalently bound to the conjugated backbone of the polyheterocycle. In this manner the polymer can be viewed as a conductive polymer/ionomer. The bound-ion is immobilized giving the polymer certain polyelectrolyte properties. In fact, *aqueous solutions* of both polythiophenes [7] and polypyrroles [8] have been prepared via this technique.

In contrast to typical polyheterocycles and analogous to ionomeric polymers, charge transport in a self-doped polymer should necessarily be controlled by the movement of only one type of ionic species (the cation) and hence interpretation of transport regimes becomes more straightforward. This specific ion transport can be attributed to the fact that the covalently bound anions, localized within the polymer matrix, will repel electrolyte anions while allowing electrolyte cations to penetrate into the film. More specifically, in solution a Donnan potential gradient exists across the film/solution interface as mobile cations diffuse from the film. This creates a small net negative charge within the film, inhibiting penetration by electrolyte anions. Since only the cations

will be mobile during oxidation and reduction, the contribution of specific ionic species to the overall charge transport performance of certain polymer can be evaluated.

Another important aspect of charge transport studies in self-doped conductive polymers is that a satisfactory description of the overall electrochemistry of conductive polyheterocycle films is not yet available. A previous treatment of polypyrrole electrochemistry considered the cyclic voltammetric currents to be mainly capacitive [9] based on theoretical simulations. Some of the assumptions implicit to this treatment have been questioned [1a]. An optoelectrochemical study of polypyrrole switching [10] concluded the process to be faradaic and controlled by Fickian diffusion of charge compensating counterions into and out of the film. Other similar treatments have also appeared [1d,11]. One study [12] examined the chronocoulometric behavior of polypyrrole films in supporting electrolyte solution and found a porous electrode model [13] to be applicable, involving essentially a capacitive behavior. Based on the assumption that charge transport is limited by counterion diffusion in polypyrrole, efforts have been made to improve their morphology by incorporation of polypyrrole into an ion specific membrane, such as Nafion, and thereby enhance charge transport rates [14,15]. It is expected that the ability to limit ion mobility to one known species in the self-doped conductive polymers will be useful in more definitively identifying the important aspects of redox charge transport.

The purpose of the present work is to compare, for the first time, the relative charge/discharge transport properties of a self-doped conductive polymer with its conjugate polyheterocycle. This is accomplished through a combination of chronocoulometric and microgravimetric techniques. We have investigated charge transport rates under well-defined conditions in order to assess the effect of electrolyte on charge transport and present the results of experiments on the redox switching of poly{pyrrole-co-[3-(pyrrol-1-yl)-propanesulfonate]} (PP-PS) in acetonitrile, containing electrolytes such as  $\text{Bu}_4\text{NBF}_4$  and  $\text{LiBF}_4$  to demonstrate the effect of ion size on charge transport. We show that, compared to polypyrrole, in the self-doped systems charge transport rates are relatively less affected by the magnitude of the applied potential step. Microgravimetric studies are used to determine the identity of the mobile ionic species. The

results obtained in these experiments are used in comparison to existing treatments of charge transport in conducting polymers.

## EXPERIMENTAL

### *Materials*

3-(pyrrol-1-yl)propanesulfonate was synthesized using a procedure reported earlier [6]. Pyrrole (Aldrich) was purified by chromatography over alumina. Acetonitrile ( $\text{CH}_3\text{CN}$ , Mallinckrodt) was Nanopure grade and was stored over activated molecular sieves prior to use. Tetrabutylammonium fluoroborate ( $\text{TBABF}_4$ ), lithium fluoroborate ( $\text{LiBF}_4$ ), and tetraethylammonium tosylate (TEATos) were dried prior to use.

### *Electrochemical Polymerization and Analysis*

Cyclic voltammetry, the electrosyntheses of the polymers and their electrochemical analyses were carried out with an EG&G Princeton Applied Research model 273 potentiostat equipped with a model 97 current interrupt IR compensation circuit.

The polypyrrole (PP) and PP-PS copolymer films used for chronocoulometric analysis were deposited on a .018  $\text{cm}^2$  platinum button working electrode from a  $5\text{-}10 \times 10^{-3} \text{ mol dm}^{-3}$  solution of pyrrole monomer and  $5\text{-}10 \times 10^{-3} \text{ mol dm}^{-3}$  equimolar solutions of the two monomers respectively, using a cyclic potential sweep (CPS) technique which has been described elsewhere [6]. In both cases, the potential of the working electrode was scanned past the potential (1.1 V vs.  $\text{Ag}/\text{AgNO}_3$ ) where the copolymerization occurs. Attempts were made to standardize the total amount of charge passed and thus the thickness of the film. Using the CPS procedure, in which the total amount of charge passed was limited to a range from 83  $\text{mC cm}^{-2}$  to 327  $\text{mC cm}^{-2}$ , polymer and copolymer films of the highest quality are obtained. The charge transport phenomena described herein are unaffected within this range of values. Scanning electron microscopy of both PP and PP-PS copolymer films show them to have identical morphologies and to be well-adhered

to the electrode surface. Separate experiments have shown that similar polymer films could be deposited using a constant current method also.

After polymerization the polymer covered working electrode was rinsed in pure  $\text{CH}_3\text{CN}$  and allowed to equilibrate in a supporting electrolyte solution prior to the chronocoulometric experiment. The solutions used for both the electropolymerization and potential step experiments as well as the  $\text{CH}_3\text{CN}$  used in rinsing the films were purged with purified  $\text{N}_2$ .

For a given polymer film, the same supporting electrolyte (e.g.,  $\text{Bu}_4\text{NBF}_4$  or  $\text{LiBF}_4$ ) used for synthesizing the film was used for the potential step experiments to avoid mixed electrolyte equilibria. For oxidative potential step experiments, the polymer film was first held at a cathodic potential for a fixed time (5 min.) to restore the electrolyte concentration in the reduced film to equilibrium values.

The potential of the electrode was then stepped oxidatively to a value greater than the peak potential for oxidation ( $E_{pa}$ ) of the film as determined by cyclic voltammetry. The charge transients obtained were stored on a Kikusui model 6520A digital storage oscilloscope. Values from the resulting charge-time curves were obtained directly from the oscilloscope via a cursor readout function and sent as an analog signal to an X-Y-t recorder for visual inspection.

The microgravimetric studies during charge/discharge of the polymer film were performed in a Vacuum Atmospheres dry box under nitrogen using an electrochemical quartz crystal microbalance (EQCM). This technique allows the mass sensing gold electrode on one face of an oscillating AT-cut quartz crystal to be used as a working electrode in a 3-electrode electrochemical cell. Thus *in-situ* mass changes associated with electrochemical processes can be determined as a function of time, charge, and potential. This arrangement has been used by various workers to study mass changes occurring at the working electrode surface as a result of an electrochemical process [16]. The ability to control and measure electrochemical parameters simultaneously with *in-situ* mass changes has also enabled the analysis of ion content and movement in conducting polymer and polymer modified electrodes [3-5]. In our studies on these conducting polyheterocycles, the EQCM system has been employed to identify the mobile ionic species upon

oxidation and reduction. Electrolytes were vacuum dried and anhydrous  $\text{CH}_3\text{CN}$  (Aldrich) was used. Polymer films were prepared potentiostatically from monomer/electrolyte solutions identical to those described above. After electropolymerization, the films were washed with  $\text{CH}_3\text{CN}$  to remove residual unreacted monomer and allowed to equilibrate in monomer free solution composed of the same electrolyte from which they were prepared.

As in the chronocoulometric studies, the potential of the electrode was stepped to a potential greater than the  $E_{\text{pa}}$  as determined by cyclic voltammetry. The resonant frequency of the oscillating quartz crystal was then measured by a Philips PM 6654 frequency counter. Simultaneously, the currents associated with the redox activity of the polymer film were monitored via a 16-bit Tecmar Labmaster data acquisition and control board. All experimental values were controlled, monitored and stored with an IBM PC-XT.

Diffuse reflectance Fourier Transform Infrared (FTIR) spectra were obtained for the copolymer grown by a constant current technique ( $\sim 1 \text{ mA cm}^{-2}$ ), using a BioRad-Digilab FTS-40 instrument. Elemental analyses were performed by Galbraith Laboratories, Inc.

## RESULTS

Cyclic voltammetric analysis of 3-(pyrrol-1-yl)propanesulfonate, hereafter termed the pyrrole sulfonate monomer, at a clean Pt electrode in an  $\text{CH}_3\text{CN}$  based electrolyte, Figure 1, shows an oxidation with a peak (a) at *ca.* 1.1 volts vs. the  $\text{Ag}/\text{AgNO}_3$ . After allowing the solution to reach quiescent equilibrium at a cathodic potential, a second scan (b) shows a much lower current than the initial. Subsequent scanning leads to a complete passivation of the electrode surface. This passivation indicates that an insoluble and electrically non-conducting or electrochemically inactive polymer film has formed which inhibits any further electroactivity. In a series of separate studies, the chemical ( $\text{FeCl}_3$ ) polymerization of the pyrrole sulfonate has been undertaken as shown in Eq. (1). Two separate fractions are obtained from this reaction: the

Equation (1)

first a black insoluble precipitate and the second a dark solution. This dark solution represents the first reported water soluble polypyrrole and will be discussed in detail elsewhere [8]. Pressed pellets of the insoluble fraction and cast films of the soluble fraction of the homopolymer poly[3-(pyrrol-1-yl)propanesulfonate] have electrical conductivities of  $10^{-8}$  to  $10^{-6}$   $\Omega^{-1}$  cm<sup>-1</sup>. This low conductivity is not surprising when compared to values found for other N-substituted polypyrroles [17] and thus poly[3-(pyrrol-1-yl)propanesulfonate] is not suitable as an electrode material as a homopolymer.

For this reason we turned our attention to copolymers of pyrrole with the pyrrole sulfonate monomer. It is well known that a continuously varied conductivity can be attained for copolymers of pyrrole with its N-substituted derivatives [18,19]. Also the most favorable dopant level (the term commonly used to denote the number of charge-balancing counter ions per pyrrole ring) ranges from 0.2 to 0.4 and copolymerization would be expected to yield a material in which a proper concentration of bound dopant ions could be attained.

Beginning with a 50/50 molar monomer feed ratio and using a constant current electropolymerization in a LiClO<sub>4</sub> electrolyte, a thick black polymeric deposit is obtained. Thorough washing with H<sub>2</sub>O, CH<sub>3</sub>CN and CH<sub>3</sub>COCH<sub>3</sub> was followed by vacuum drying and analysis. The FTIR spectrum of the copolymer was compared with that of polypyrrole and poly[3-(pyrrol-1-yl)propanesulfonate]. Strong S-O stretching bands at *ca.* 1200 cm<sup>-1</sup>, seen in both poly[3-(pyrrol-1-yl)propanesulfonate] and the PP-PS copolymer, were used to establish the presence of the sulfonate ion in the materials [20]. Elemental analyses were carried out to determine copolymer composition: Anal. Found (Calcd): C, 52.42 (54.60); H, 4.10 (4.58); N, 12.84 (12.76); S, 8.76 (9.64); Cl, 0.15 (0.16); Li, 0.70 (0.70); K, 0.36 (0.36). A water content of 2.67% was determined by a Karl Fisher titration. The calculated values approximate the structure shown in Structure 1. The slight error in these values can be attributed to the complicated nature of electrochemically synthesized conductive polymers, but a general evaluation can be made.

Structure 1

Using a 50/50 monomer feed ratio there is about 1 pyrrole sulfonate monomer incorporated for every 2 unsubstituted pyrroles along the polymer chain as desired for the most beneficial doping level. It is expected that the substituted and unsubstituted pyrroles are distributed along the polymer chain in a random fashion since the polymerization mechanism requires an initial electrochemical oxidation of each monomer. The pyrrole sulfonate monomer is incorporated into the copolymer at a slower rate than the unsubstituted pyrrole due to its slightly higher (*ca.* 200 mV) oxidation potential.

It can be seen that, in this polymer, in the oxidized form, the bound sulfonates exist in two types of environments. Approximately 2/3 are involved with compensating positive charge on the polymer backbone, while the remaining pendant ions are associated with either Li<sup>+</sup>, K<sup>+</sup> or possibly H<sup>+</sup>. The low K<sup>+</sup> content can be attributed to residual potassium sulfonate groups from the initial monomer. The low ClO<sub>4</sub><sup>-</sup> content shows there to be little free dopant ion even though the polymer is in the doped state. These results do indicate that a self-doped copolymer, in which the bound sulfonate is serving as the dopant ion, has formed and a fractional charge of +0.215 per pyrrole ring is delocalized along the polymer backbone and is being compensated by the bound sulfonate ions. The cyclic voltammogram (CV) for the redox reaction of the copolymer poly{pyrrole-co-[3-(pyrrol-1-yl)propanesulfonate]} (PP-PS) in acetonitrile containing 0.1M (LiBF<sub>4</sub>) is shown in Figure 2 with the CV for polypyrrole (PP) in the same medium for comparison. The apparent oscillations in the CV of the copolymer are due to the current interrupt iR compensation technique employed. Both CV's show the oxidation of the polymer as a distinct peak while the reduction peak is only visible for polypyrrole, and is masked by background (or capacitive charging) current for the copolymer. The more positive value of the E<sub>pa</sub> for the copolymer as compared to polypyrrole, and the larger peak width suggest slower electron transfer and a range of E<sub>o</sub>' values. This is not surprising considering the inherent disorder within these relatively amorphous polymers which can yield a range of energy states to which electron transfer can occur.

Pressed pellet conductivity measurements on the copolymer yielded a value of *ca.* 10<sup>-2</sup> Ω<sup>-1</sup> cm<sup>-1</sup>, intermediate between the two homopolymers. Electrochemical oxidations such as

ferrocene to ferrocenium ion proceed smoothly at the PP-PS electrode showing that it is conductive and suitable as an electrode material.

Chronocoulometric experiments were carried out for the redox reactions of the PP-PS copolymer and polypyrrole in 0.1M TBABF<sub>4</sub> and 0.1M LiBF<sub>4</sub> in acetonitrile. These electrolytes were chosen because of the large differences in cation size [21]. A double potential step program was employed with the initial potential in the fully reduced or cathodic region, being chosen from the cyclic voltammograms. The time window for the forward electrolysis was chosen to be < 2s in order to ensure semi-infinite conditions. The minimal film thickness required to ensure semi-infinite conditions should be greater than the diffusion layer thickness ( $\delta$ ). From the equation  $\delta=(2Dt)^{1/2}$ , where  $D\sim 1 \times 10^{-10} \text{ cm}^2 \text{ s}^{-1}$  and  $t=2\text{s}$ , the diffusion layer thickness equals 0.2  $\mu\text{m}$ . Assuming a relationship of 233  $\text{mC } \mu\text{m}^{-1} \text{ cm}^{-2}$ , a 0.2  $\mu\text{m}$  thick film would require 48  $\text{mC cm}^{-2}$  of charge during film formation. This is exceeded by all films studied, as shown in Table 1 ( $Q_{\text{film}}$ ). Although it has been shown that the time required for complete oxidation or reduction for most conducting polymers can be as long as 20 minutes [1a], the mobile species can easily encounter a boundary at much shorter times. When this occurs obvious deviations from linearity are evident, in log-log plots of charge (Q) vs. time (t), which are not seen in our data. The data from chronocoulograms are displayed as log-log plots in Figures 3 and 4. Such a representation is more informative than a charge versus  $t^{1/2}$  plot. The slopes of the lines show that the dependence of charge on time is not  $t^{1/2}$  as expected for Cottrell behavior but rather as  $t^\alpha$  where we find  $0.2 < \alpha < 0.8$ . This result is typical of irregular electrode surfaces [22]. A close inspection of these results show a small deviation from linearity. This may be attributed to subtle morphological defects which complicate these systems and allow some of the mobile species to encounter boundaries at short times.

Comparison of the results in Figure 4 on two PP-PS copolymers films of approximately the same thickness (100  $\text{mC cm}^{-2}$  vs. 83  $\text{mC cm}^{-2}$  used during electrosynthesis) details another important feature; the higher rate of charge passage for the PP-PS electrode in LiBF<sub>4</sub> as compared to TBABF<sub>4</sub>, reflects the effect of the cationic size on the rates ( $\text{Li}^+$ ,  $r=0.068 \text{ nm}$ ;  $\text{TBA}^+$ ,  $r=0.513$

nm) [2a]. This is the expected result for the self-doped copolymer if ion-specific transport is occurring, since the smaller cation ( $\text{Li}^+$ ) is more mobile. It should be noted that the ions are most likely solvated to some extent under these experimental conditions precluding any direct treatment of ion size. Relative interactions of the mobile ionic species with the bound sulfonate anions can be compared. For polypyrrole, the behavior may be more complex because either the cation or anion can be the mobile species. The amount of charge passed through the film after 1 s [ $Q_t(t=1\text{s})$ ] in the potential step experiment is used to estimate the relative rates of transport. The relevant parameters are shown in Table I.

The potential step experiment described above was also repeated with variation in the magnitude of the voltage jump. The potential of the working electrode was stepped to various potentials ( $E_f$ ) beyond the oxidation peak potential ( $E_p$ ) and the data from the resulting chronocoulograms were analyzed to obtain the value  $Q_t(t=1\text{s})$  as a function of the potential difference applied to the polymer ( $E_f - E_p$ ). This is shown in Figure 5. The parameter  $E_f - E_p$  has been used previously to monitor potential difference effects on ion transport beyond the diffusion-limited region [12]. The significant difference between polypyrrole and PP-PS in the response to the step size increment is immediately apparent. The implications are discussed below.

The specific identification of the mobile ionic species during charge/discharge of conductive polymers is critical to understanding the transport data presented. For example, a brief investigation of this has been carried out by Miller [2b] on polypyrrole. Analysis of films by both XPS and atomic absorption spectroscopy after reduction indicated the identity of the mobile anion is controlled by both anion type and what solvent was used. The use of a quartz crystal microbalance [3-5] allows *in-situ* examination of this process and can dynamically monitor the mass changes occurring in these films.

This is illustrated for polypyrrole and the pyrrole/pyrrole sulfonate copolymer in Figures 6 and 7. The general appearance of the frequency vs. time curve is similar to a typical chronocoulometric curve and indeed analogies may be made between them. The QCM has been used for many years to determine mass changes ( $\Delta m$ ) in a vacuum by monitoring changes in the

resonant frequency of an oscillating quartz crystal by using the Sauerbrey equation:

$$\Delta f = -2f_0^2 \Delta m / A (\rho_q \mu_q)^{1/2} \quad (2)$$

where  $f_0$ =resonant frequency of the unloaded quartz crystal sandwiched between two metallic electrodes,  $\rho_q$ =density of the quartz =2.648 g cm<sup>-3</sup>,  $\mu_q$ =shear modulus of quartz =2.947x10<sup>11</sup>, A=surface area of electrode or film, and  $\Delta m$ =mass change in grams [23]. Recent work has shown that when one face of an AT-cut quartz crystal is immersed in a liquid, the crystal will continue to oscillate with a frequency shift given by the equation:

$$\Delta f_0 = f_0^{3/2} (\rho_l \eta_l / \pi \rho_q \mu_q)^{1/2} \quad (3)$$

where  $\rho_l$  and  $\eta_l$  are the density and absolute viscosity of the liquid overlayer, respectively [24,25]. In order to quantitatively apply the Sauerbrey equation to a polymer film in solution, the film must behave as a rigid, perfectly elastic overlayer. Studies on several polymer systems including polypyrrole indicate that this rigid film approximation is valid if the polymeric overlayer thickness is small compared to the thickness of the crystal and if the overall mass loading results in a frequency change that is negligible with respect to the resonant frequency of the unloaded crystal [3a,4,5,26]. Although we believe this to be valid in our systems, only the qualitative nature of the Sauerbrey equation will be examined in this paper.

Figures 6a and 6b show the effect of the application of sequential oxidative/reductive steps to both the polypyrrole and the copolymer films equilibrated in TBABF<sub>4</sub> electrolyte at an initial reductive potential. An increase in frequency (decrease in mass) is observed upon oxidation while a decrease in frequency (increase in mass) is observed upon reduction. This can be attributed to the respective expulsion and insertion of cations within the polymer matrix. It is quite possible, and even expected, that these polymer films are swollen with the solvent/electrolyte solution. During electrochemical switching the oxidation level of the polymer is being changed. For example, upon oxidation a delocalized cation spanning a few pyrrole units is created. Though the composition within the polymer matrix may be quite complicated, mass fluxes can be attributed to ion movement (with possible associated solvent molecules) required to maintain charge neutrality

within the film. Thus, in this electrolyte system the cation is the mobile species for both polymer types.

The same experiment performed with TEATos as the supporting electrolyte is shown in Figures 7a and 7b. It is evident that in the homopolymer of pyrrole the transport of mass is complicated. Upon oxidation, an initial mass loss is observed followed by mass gain over most of the experiment. This suggests that after an initial fast expulsion of electrolyte cations, tosylate anions diffuse into the film in order to conserve charge. The reductive step of PP in this medium shows the opposite behavior. After an initial insertion of electrolyte cations, tosylate ions are able to diffuse out of the polymer, leaving behind a neutral film.

Examination of the self-doped copolymer/TEATos system shows that just as in the TBABF<sub>4</sub> case, the cation is the only mobile species. An important aspect of these comparisons is the similarities in physical nature of the PP and PP-PS films. As mentioned earlier, electron microscopic examination of films synthesized in this manner showed them to be equivalent, completely covering the metallic electrodes underneath. These results are as expected for a bound dopant ion conducting copolymer in which the mobile species possible is the cation, as will be discussed further below.

## DISCUSSION

The movement of charge during the redox switching of electroactive polymers during a potential perturbation [27] has been treated as a composite process involving hopping of electrons between adjacent pairs of oxidized and reduced sites, equivalent to a diffusion of electrons with a concurrent diffusion of charge compensating counterions which can often be rate-limiting [28]. The ion transport in such a situation can be visualized as Fickian with an appropriate finite diffusion equation to describe it [29]. Relative transport comparisons can be made by monitoring the charge passed ( $Q_c$ ) after a short time of oxidation or reduction. This type of analysis has also been applied to the redox switching of conducting polymers like polypyrrole [12]. However, the difficulty involved here is the significant contribution of capacitive charging to the total charge

consumed. The Feldberg model in fact emphasizes the capacitive contribution to the switching process [9]. According to this model, the total charge,  $Q_T$ , passed during the cyclic voltammetric oxidation of polypyrrole can be expressed as,

$$Q_T = Q_C + Q_F \quad (4)$$

where  $Q_C$  is the capacitive charge given by

$$Q_C = a(E - E_{ZC})Q_S \quad (5)$$

$E_{ZC}$  is the potential of zero charge,  $Q_F$  is the faradaic contribution,  $a$  is a constant and  $Q_S$  is the coulombs of oxidized polypyrrole per unit area. Thus a cyclic voltammogram, calculated with an appropriate equation for  $i_F = (dQ_F/dt)$ , using the treatments for surface species [30] can be constituted by essentially capacitive currents beyond the peak region. Feldberg has simulated cyclic voltammograms whose shapes are similar to the experimentally observed cyclic voltammograms for polypyrrole. However, a large capacitance for the electrode requires a high surface to volume ratio and a high density of surface energy states. This assumption has been questioned [1a]. The alternative is a combination of faradaic and capacitive components in which case the current would be limited by mass transport. A recent study by Tanguy and Mermilliod [31] in which a.c. impedance and cyclic voltammetry techniques were used to separate the capacitive and non-capacitive components of charge support this claim.

In the case of the self-doped polypyrrole discussed here, the broad CV, as shown in Figure 2, suggests a range of  $E_0'$  values and thus the currents observed in the switching process can be significantly faradaic over a large range of potential. This leads to a continuous removal of electrons from the  $\pi$  system of the polymer and complicates the distinction between faradaic and double layer charge. This has also been proposed for the case of polyaniline [32] where it has been suggested that the highest occupied  $\pi$  orbital of aniline is broadened into a one-dimensional band. Recent quantitative QCM results of mass transport in polypyrrole films during cyclic voltammetry suggest that true faradaic (processes accompanied by mass transport and charge compensation) and capacitive (processes not accompanied by mass transport) components can be separated [33].

The porous electrode model for polypyrrole [12] electrochemistry relies partly on the Feldberg model. Therefore, although the results shown in Figure 5 do confirm that, in polypyrrole, charge transport is potential dependent, it is important to realize that this behavior could come about, simply as a result of the migration of counterions into the film for the charge compensating process without requiring a rigorous application of the porous electrode model such as that shown for carbon electrodes [13]. This treatment is based on the assumption of negligible faradaic currents which is highly questionable in the case of polypyrrole.

Hence, it seems more reasonable to treat the chronocoulometric behavior of polypyrrole as being due to a combination of diffusional and migrational processes. Based on the argument above for the copolymer (PP-PS) behavior, we see, from the data of Figure 5, that a similar model is appropriate in describing the charge transient behavior. The lower sensitivity of the chronocoulometric slopes in the copolymer to the size of the potential step indicates lower mobilities for the charge carriers (ions) in the film. This can most likely be attributed to ion pairing of the mobile cations to the bound sulfonate ions. This could also arise from the fact that the movement of the ionic species involved is not charge-compensating. Instead the covalently bound dopant ions are distributed along the conjugated polymer backbone and can stabilize the delocalized cation with very little necessary movement. Thus we have shown that  $Q_t$ , at short times ( $<2s$ ), represents a meaningful comparative rate constant for the important kinetic parameter of charge transport.

Actual separation of the diffusional and migrational components to charge transport is difficult in these materials. This problem has been treated theoretically [34]. The fact that a doubling of the overpotential in these films, see Table 1, leads to an increase in charge passed of about 1.5 times in both cases suggests comparable contributions of diffusion and migration.

The mechanism for self-doping or charge compensation is outlined schematically in Figure 8 where the curved double lines represent the conjugated polyheterocycle backbone. Upon oxidation the free cations are expelled from their position as counter ion to the bound anion.

Reduction of the polymer film releases the bound anion from the charged site on the chain and the free cation diffuses back to compensate the charge of the bound anion.

Thus, in contrast to the case of polypyrrole the charge compensating doping process is necessarily separated from the ion movement. This is exemplified by the microgravimetric results of Figure 7 where the TEA<sup>+</sup> ion is definitely the mobile species during charge/discharge of the PP-PS copolymer, but its identity is more complicated in the parent polypyrrole.

A separate observation of the relative rates of oxidation and reduction in the self-doped copolymers indicated a significantly faster reductive process. Ion pairing of the bound sulfonate anion to the mobile cation in the neutral (reduced) form of the polymer inhibits transport during oxidation relative to the ability of free cations to diffuse from solution back to the bound anions during reduction.

The slopes of the plots in Figures 3 and 4, especially those for the PP-PS film are not exactly equal to 0.5, as would be expected for perfect Cottrell behavior. This could be due to the irregular morphology of the polymer leading to a 'rough' electrode surface. The DeLevie treatment [22] if applied to the PP-PS electrode would predict varying values for  $\alpha$ .

## CONCLUSIONS

In conclusion, we have compared the rates of redox processes for the homopolymer, polypyrrole, and the self-doped copolymer, poly{pyrrole-co-[3-(pyrrol-1-yl)propanesulfonate]}. Elemental analysis confirms that doping in the copolymer is mainly achieved through the sulfonate anion that is covalently bound to the substituted nitrogens in the polymer chains.

Chronocoulometric data indicates that charge transport is faster in the pyrrole homopolymer than in the copolymer and is sensitive to cation size. Furthermore, reduction in the copolymer is faster than oxidation due to ion pairing effects between the sulfonate anion and mobile cation. The deviation from ideal Cottrell behavior seen in the charge vs. time data is a result of the irregular polymeric electrode surface which was observed by electron microscopy. Microgravimetric data,

utilizing a quartz crystal microbalance, confirms that the mobile ionic species is the cation in the copolymer, while polypyrrole exhibits a complex behavior that is dependent on the cation identity.

#### ACKNOWLEDGMENTS

The authors would like to acknowledge the many stimulating discussions with Dr. T. Pajkossy and Professor K. Rajeshwar. Comments from one referee concerning the separation of diffusional and migrational contributions to charge transport are greatly appreciated. Financial support through a grant from the Defense Advanced Research Projects Agency monitored by the Office of Naval Research, the Texas Advanced Technology Research Program, the donors to the Petroleum Research Fund Administered by the American Chemical Society and the Robert A. Welch Foundation is gratefully acknowledged.

## REFERENCES

- 1 (a) B.J. Feldman, P. Burgmayer, R.W. Murray, *J. Am. Chem. Soc.*, 107 (1985) 872. (b) L.L. Miller, B. Zinger, Q.X. Zhou, *J. Am. Chem. Soc.*, 109 (1987) 2267. (c) B. Zinger, L.L. Miller, *J. Am. Chem. Soc.*, 106 (1984) 6861. (d) E.M. Genies, J.M. Pernaut, *Synthetic Metals*, 10 (1984/85) 117. (e) R.A. Bull, F.F. Fan, A.J. Bard, *J. Electrochem. Soc.*, 129 (1982) 1009.
- 2 (a) P. Marque, J. Roncali, F. Garnier, *J. Electroanal. Chem.*, 218 (1987) 107.  
(b) Q.X. Zhou, C.J. Kolaskie, L.L. Miller, *J. Electroanal. Chem.*, 223 (1987) 283.  
(c) R.L. Blankespoor, L.L. Miller, *J. Chem. Soc., Chem. Commun.* (1985) 90.
- 3 (a) J.H. Kaufman, K.K. Kanazawa, G.B. Street, *Phys. Rev. Lett.*, 26 (1984) 2461.  
(b) C.K. Baker, J.R. Reynolds, *Polymer Prepr. (Am. Chem. Soc., Div. Polym. Chem.)*, 28 (1987) 284.
- 4 D.A. Buttry, D. Orata, *J. Am. Chem. Soc.*, 109 (1987) 3574.
- 5 P.T. Varineau, D.A. Buttry, *J. Phys. Chem.*, 91 (1986) 1292.
- 6 N.S. Sundaresan, S. Basak, M. Pomerantz, J.R. Reynolds, *J. Chem. Soc., Chem. Commun.* (1987) 621.
- 7 (a) A.O. Patil, Y. Ikenoue, F. Wudl, A.J. Heeger, *J. Am. Chem. Soc.*, 109 (1987) 1858.  
(b) A.O. Patil, Y. Ikenoue, N. Basescu, N. Colaneri, J. Chen, F. Wudl, A.J. Heeger, *Synth. Met.*, 20 (1987) 151.
- 8 J.R. Reynolds, M. Pomerantz, Y.J. Qiu, S. Basak, unpublished results.
- 9 S.W. Feldberg, *J. Am. Chem. Soc.*, 106 (1984) 4671.
- 10 E.M. Genies, G. Bidan, A.F. Diaz, *J. Electroanal. Chem.*, 149 (1983) 101.
- 11 R.W. Murray, *Philos. Trans. Roy. Soc. Lond.*, A302, (1981) 253.
- 12 P.G. Pickup, R.A. Osteryoung, *J. Electroanal. Chem.*, 195 (1985) 271.
- 13 A.M. Johnson, J. Newman, *J. Electrochem. Soc.*, 118 (1971) 510.
- 14 G. Nagasubramanian, S. DiStefano, J. Moacanin, *J. Phys. Chem.*, 90 (1986) 4447.
- 15 R.M. Penner, C.R. Martin, *J. Electrochem. Soc.*, 133 (1986) 2206.

- 16 (a) T. Nomura, O. Hatori, *Analytica Chimica Acta*, 115 (1980) 323. (b) S. Bruckenstein, M. Shay, *J. Electrochim. Acta*, 188 (1985) 131. (c) S. Bruckenstein, S.J. Swarthirajan, *Electrochim. Acta*, 30 (1985) 851. (d) R. Schumacher, K.K. Kanazawa, G. Borges, *Surf. Sci.*, 163 (1985) L621. (e) M. Benje, M. Eiermann, U. Pittermann, K.G. Weil, *Ber. Bunsenges. Phys. Chem.*, 90 (1986) 435. (f) O. Melroy, R. Schumacher, J.G. Gordon, *J. Electroanal. Chem.*, 216 (1987) 127. (g) O. Melroy, E.S. Grabbe, R.P. Buck, *J. Electroanal. Chem.*, 223 (1987) 67.
- 17 A.F. Diaz, J.I. Castillo, J.A. Logan, W.Y. Lee, *J. Electroanal. Chem.*, 129 (1981) 115.
- 18 K.K. Kanazawa, A.F. Diaz, M.T. Krounbi, G.B. Street, *Synth. Met.*, 14 (1981) 119.
- 19 J.R. Reynolds, P.A. Poropatic, R.L. Toyooka, *Macromolecules*, 20 (1987) 958.
- 20 J.G. Graselli, W.M. Ritchey (Eds.), *Atlas of Spectral Data and Physical Constants of Organic Compounds*, CRC Press Inc., Cleveland, 1975.
- 21 H.S. Harned, B.B. Owen in *The Physical Chemistry of Electrolytic Solutions*, Ch. 6, Reinhold, New York, 1958 .
- 22 R. DeLevie in P. Delahay, C.W. Tobias (Eds.), *Advances in Electrochemistry and Electrochemical Engineering*, Vol. 6, Wiley, New York, 1967, p. 329.
- 23 G. Sauerbrey, *Z. fur Phys.* 155 (1959) 206.
- 24 K.K. Kanazawa, J.G. Gordon, *Anal. Chem.*, 57 (1985) 1770.
- 25 K.K. Kanazawa, J.G. Gordon, *Analyt. Chem. Acta*, 175 (1985) 99.
- 26 K.K. Kanazawa, preprint.
- 27 R.W. Murray in A.J. Bard (Ed.), *Electroanalytical Chemistry*, Vol. 13, Marcel Dekker, New York, 1984.
- 28 F.B. Kaufman, A.H. Schroeder, E.M. Engler, S.R. Kramer, J. Q. Chambers, *J. Am. Chem. Soc.*, 102 (1980) 483.
- 29 R.W. Murray, P. Daum, *J. Phys. Chem.*, 85 (1981) 389.
- 30 E. Laviron in A.J. Bard (Ed), *Electroanalytical Chemistry*, Vol. 12, Marcel Dekker, New York, 1982 .

- 31 J. Tanguy and N. Mermilliod, *Synth. Met.*, 21 (1987) 129.
- 32 S. H. Glarum and J. H. Marshall, *J. Phys. Chem.*, 90 (1986) 6076.
- 33 C. K. Baker and J. R. Reynolds, unpublished results.
- 34 W. T. Yap, R. A. Durst, E. A. Blubaugh and D. D. Blubaugh, *J. Electroanal. Chem.* 144 (1983) 69.

TABLE I

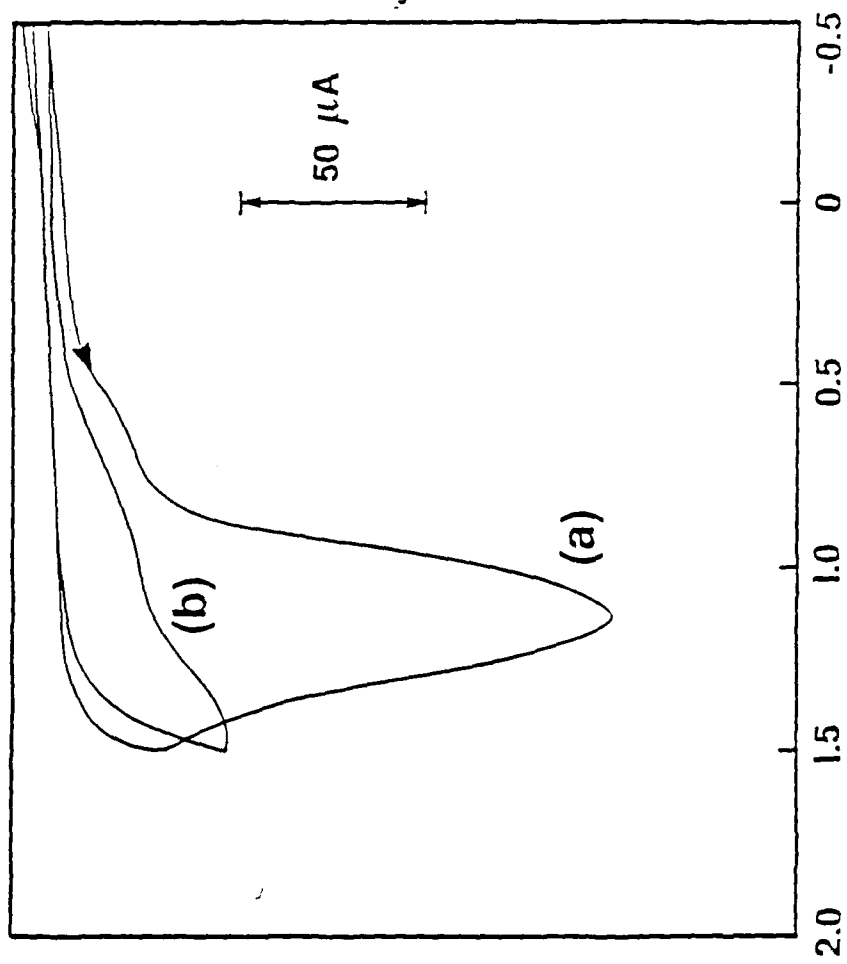
## Charge Transport Parameters

| Polymer         | Electrolyte <sup>a</sup> | $E_{pa}$ (volts) <sup>b</sup> | $E_F E_p$ (volts) | $\alpha$ | $Q_i(t=1s)$<br>( $\mu C$ ) | $Q_{film}$<br>( $mC\ cm^{-2}$ ) <sup>c</sup> |
|-----------------|--------------------------|-------------------------------|-------------------|----------|----------------------------|--|
| polypyrrole     | TBABF <sub>4</sub>       | 0.0                           | 0.05              | 0.52     | 213                        | 327  |
|                 |                          |                               | 0.10              | 0.58     | 305                        |  |
|                 |                          |                               | 0.15              | 0.54     | 357                        |  |
|                 |                          |                               | 0.20              | 0.55     | 450                        |  |
| polypyrrole     | LiBF <sub>4</sub>        | 0.0                           | 0.15              | 0.72     | 565                        | 177  |
|                 |                          |                               | 0.20              | 0.92     | 631                        |  |
| PP-PS copolymer | TBABF <sub>4</sub>       | 0.20                          | 0.20              | 0.70     | 36                         | 100  |
|                 |                          |                               | 0.30              | 0.65     | 48                         |  |
|                 |                          |                               | 0.40              | 0.64     | 57                         |  |
| PP-PS copolymer | LiBF <sub>4</sub>        | 0.05                          | 0.20              | 0.56     | 61                         | 83   |
|                 |                          |                               | 0.35              | 0.30     | 85                         |  |
|                 |                          |                               | 0.45              | 0.27     | 91                         |  |
|                 |                          |                               | 0.75              | 0.50     | 156                        |  |

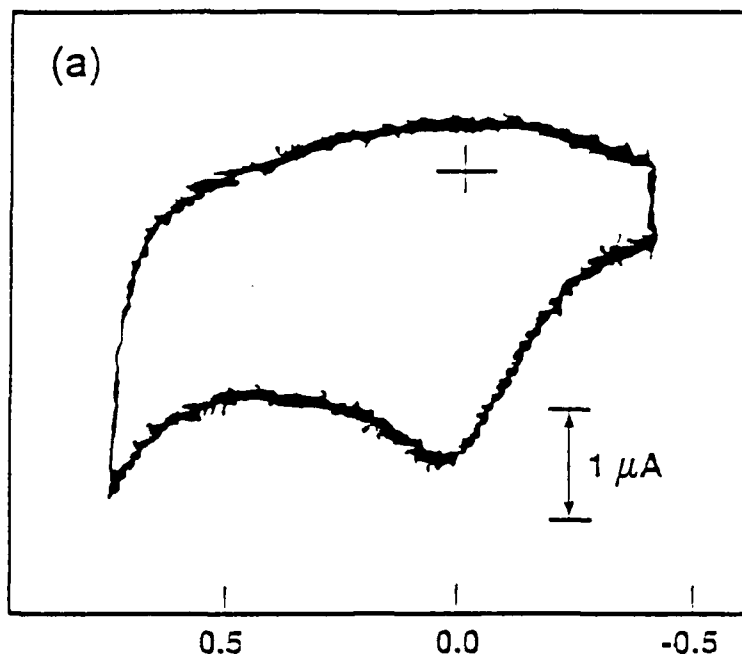
<sup>a</sup>The solvent used was acetonitrile. <sup>b</sup>Volts versus Ag/Ag<sup>+</sup> (0.1M). <sup>c</sup>Area of Pt electrode was 0.018 cm<sup>2</sup>.

## FIGURE CAPTIONS

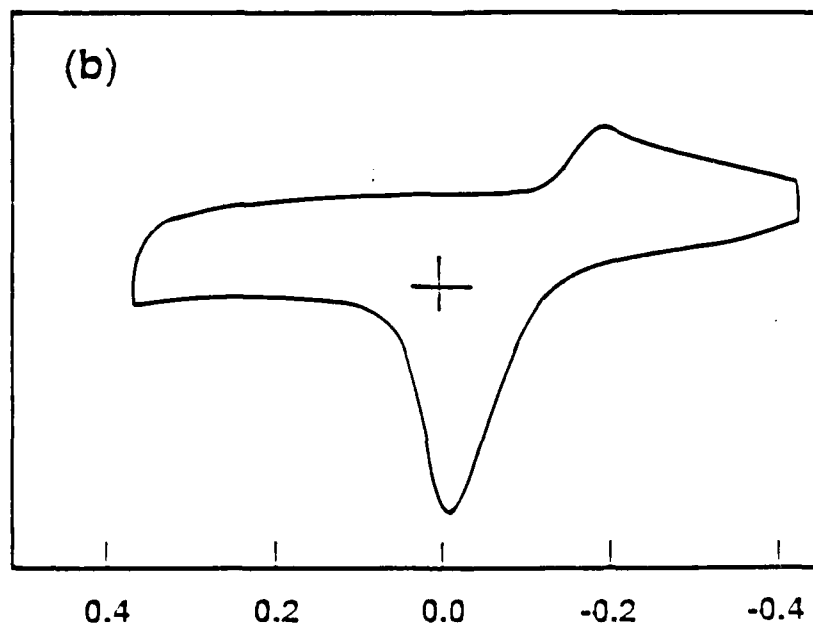
- Figure 1: Cyclic voltammogram for the oxidation of 3-(pyrrol-1-yl)propanesulfonate at a Pt button working electrode. Medium: 0.1M TBABF<sub>4</sub> in MeCN. Scan rate 100 mV/s. Potentials are vs. Ag/Ag<sup>+</sup> (0.1M). A = 0.018 cm<sup>2</sup>
- Figure 2: Cyclic voltammogram for the redox reaction of (a) PP-PS copolymer in 0.1M LiBF<sub>4</sub>/MeCN medium, (b) polypyrrole in 0.1M LiBF<sub>4</sub>/MeCN. Scan rate 100 mV/s. Potential vs. Ag/Ag<sup>+</sup> (0.1M). A = 0.018 cm<sup>2</sup>
- Figure 3: Log-log plots for the charge-time transients for polypyrrole, (□) LiBF<sub>4</sub> electrolyte, E<sub>f</sub>-E<sub>p</sub> = 0.15V (○) LiBF<sub>4</sub> electrolyte, E<sub>f</sub>-E<sub>p</sub> = 0.10V (◇) TBABF<sub>4</sub> electrolyte, E<sub>f</sub>-E<sub>p</sub> = 0.15V (△) TBABF<sub>4</sub> electrolyte, E<sub>f</sub>-E<sub>p</sub> = 0.10V.
- Figure 4: Log-log plots for the charge-time transients for poly{pyrrole-co-[3-(pyrrol-1-yl)propanesulfonate]}, (□) LiBF<sub>4</sub> electrolyte, E<sub>f</sub>-E<sub>p</sub> = 0.50V (○) LiBF<sub>4</sub> electrolyte, E<sub>f</sub>-E<sub>p</sub> = 0.40V (◇) TBABF<sub>4</sub> electrolyte, E<sub>f</sub>-E<sub>p</sub> = 0.50V (△) TBABF<sub>4</sub> electrolyte, E<sub>f</sub>-E<sub>p</sub> = 0.40V.
- Figure 5: Plot of Q<sub>t</sub>(t=1s) for the chronocoulometric log-log plots vs. E<sub>f</sub>-E<sub>p</sub> (□) PP, LiBF<sub>4</sub> electrolyte (○) PP, TBABF<sub>4</sub> electrolyte (◇) PP-PS, LiBF<sub>4</sub> electrolyte (△) PP-PS, TBABF<sub>4</sub> electrolyte.
- Figure 6: Quartz crystal microbalance analysis of oxidation followed by reduction in TBABF<sub>4</sub> electrolyte. (a) polypyrrole (b) poly{pyrrole-co-[3-(pyrrol-1-yl)propanesulfonate]}
- Figure 7: Quartz crystal microbalance analysis of oxidation followed by reduction in TEATOS electrolyte. (a) polypyrrole (b) poly{pyrrole-co-[3-(pyrrol-1-yl)propanesulfonate]}
- Figure 8: Schematic of oxidation/reduction processes in self-doped conductive polymers.



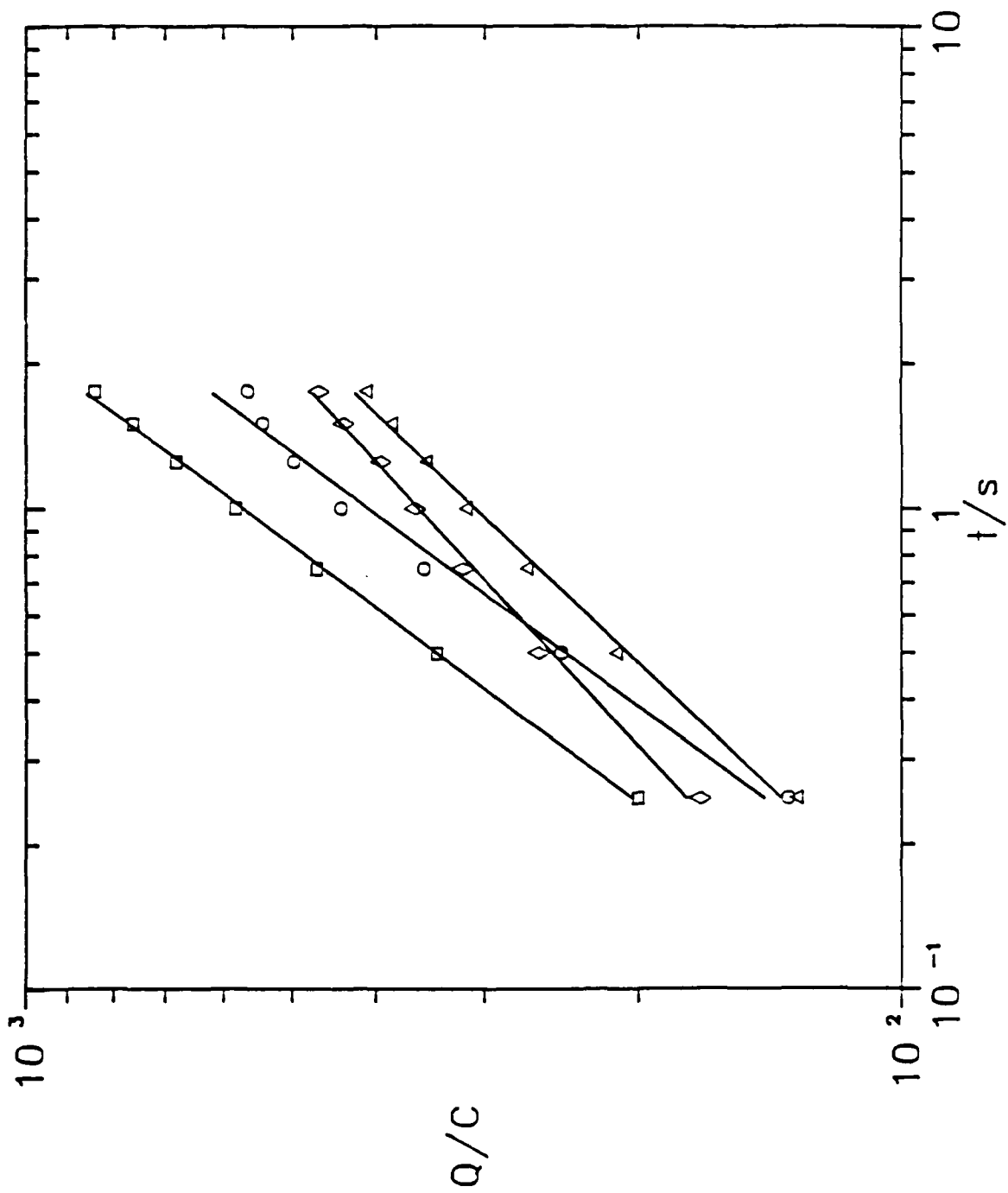
E (volts) vs. Ag/Ag<sup>+</sup> (0.1M)

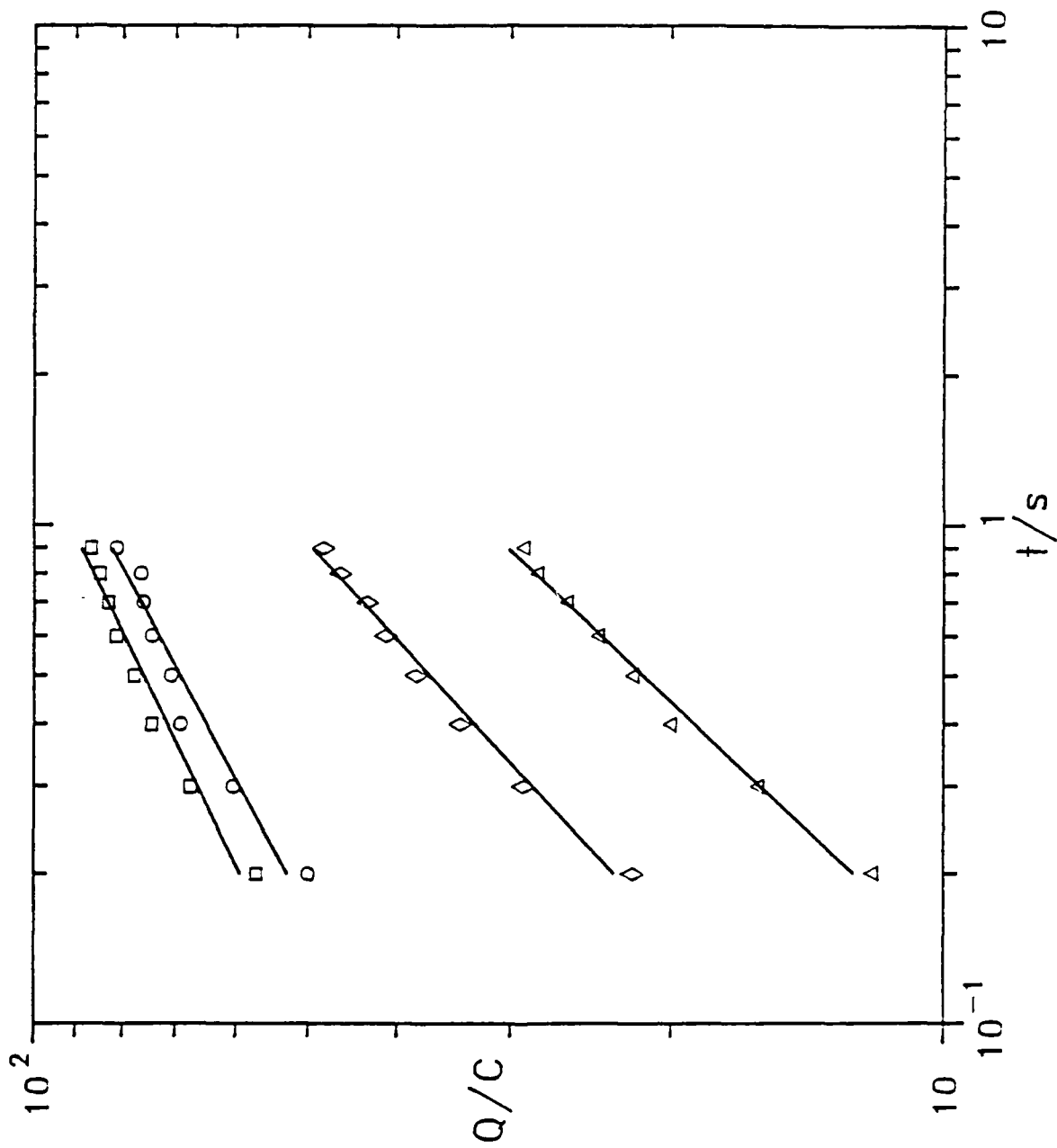


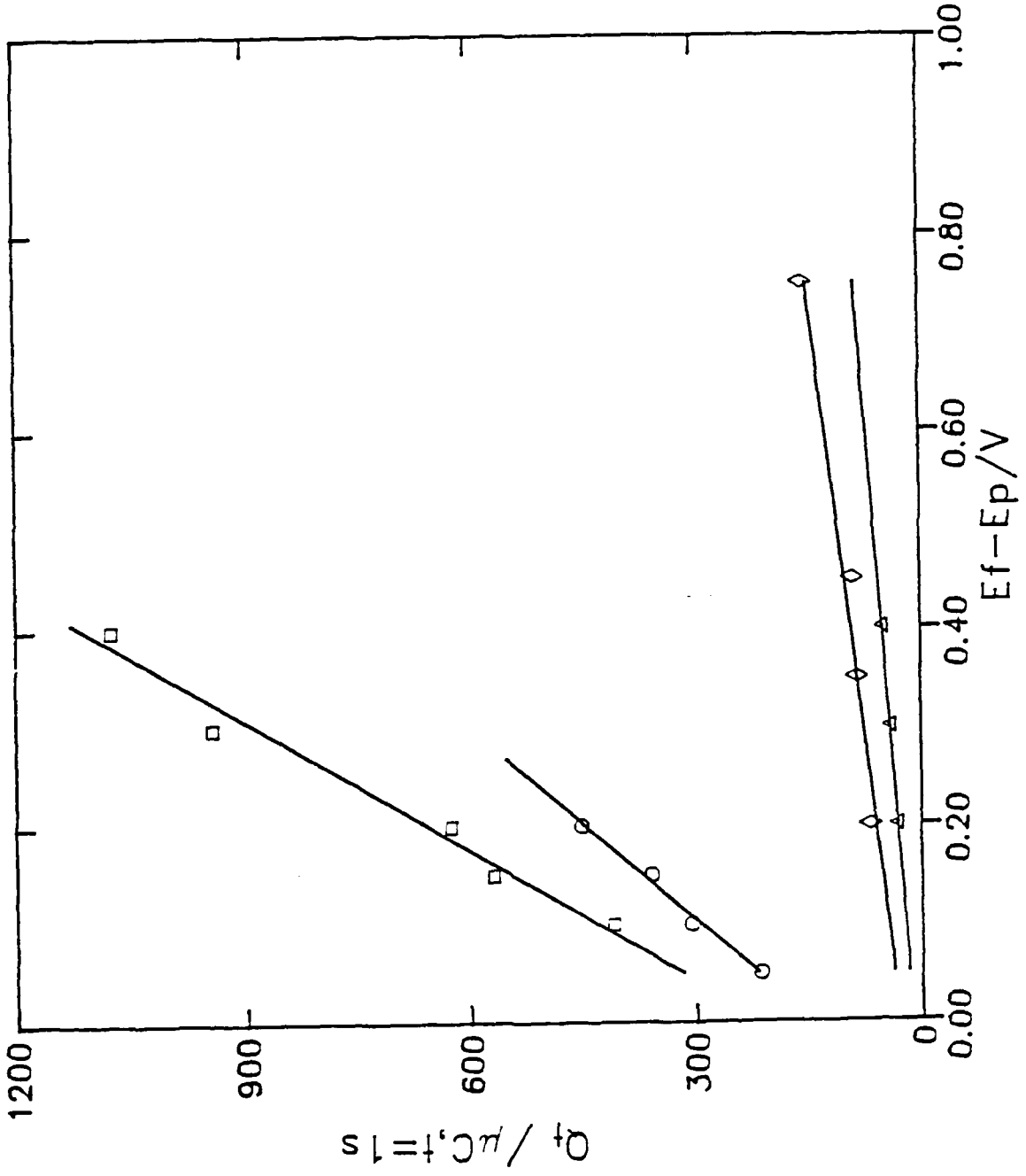
E (volts) vs. Ag/Ag<sup>+</sup> (0.1M)

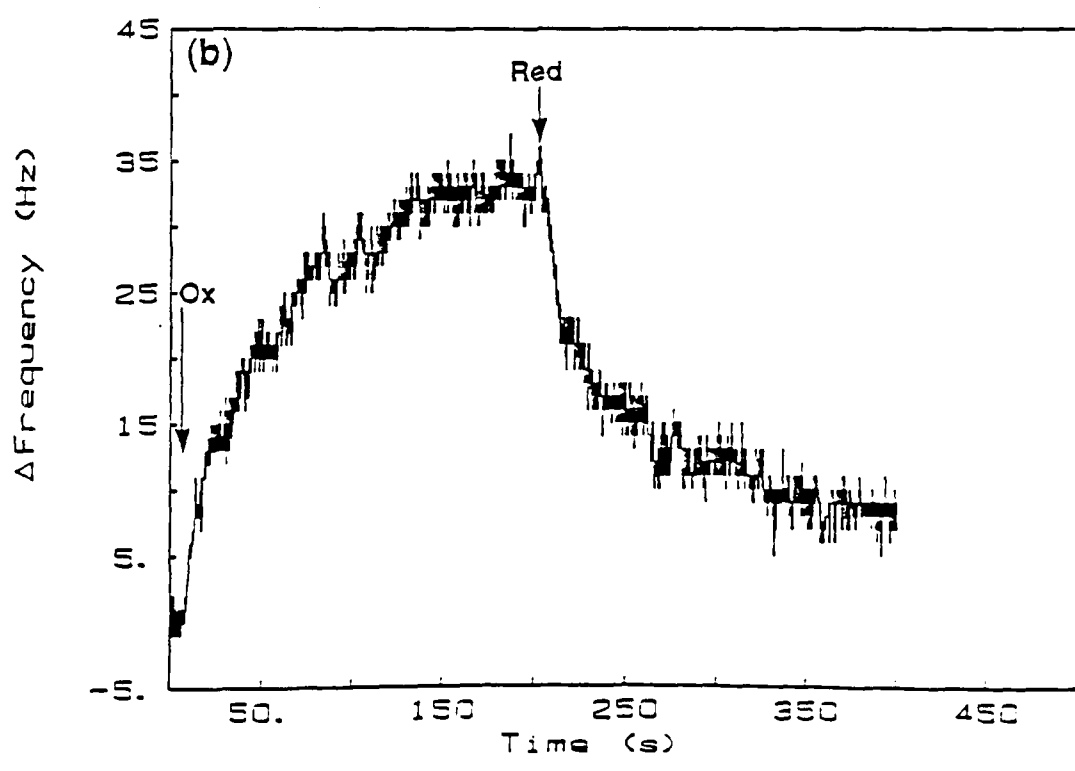
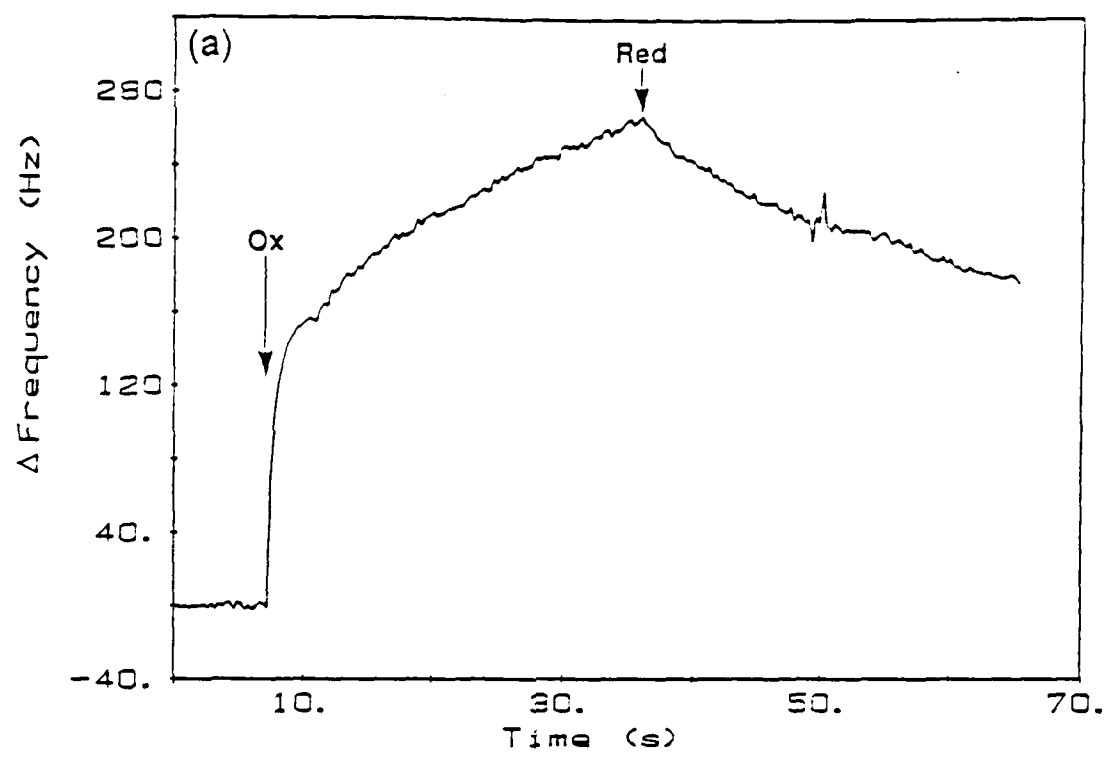


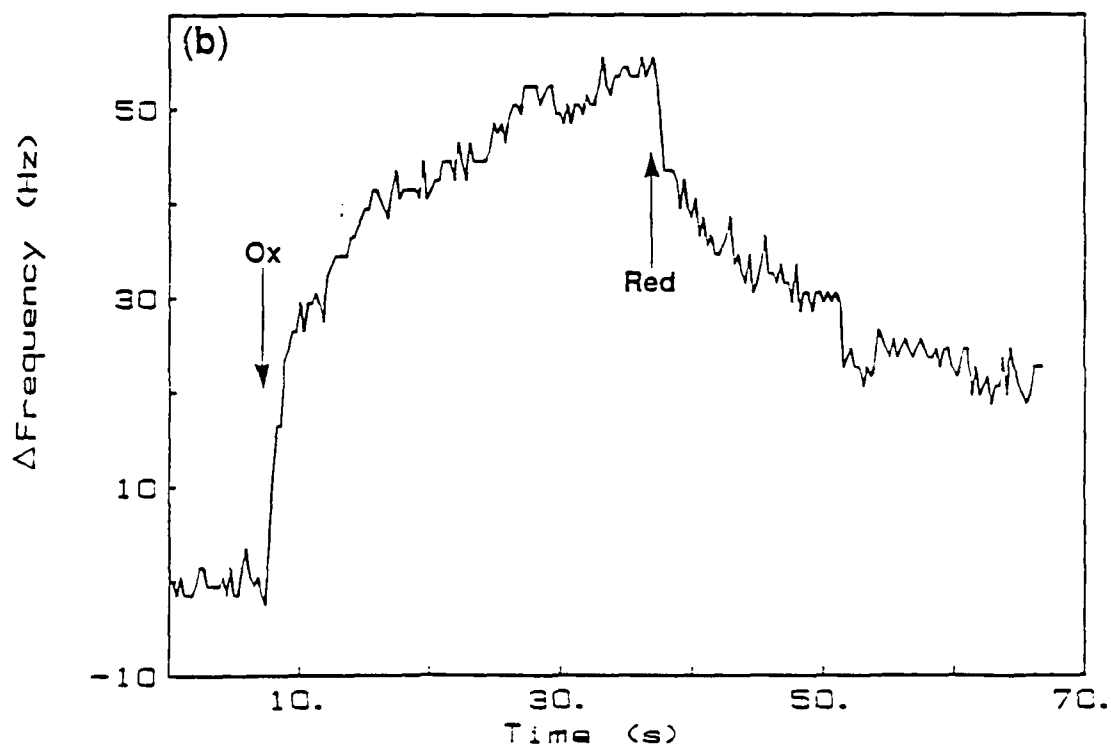
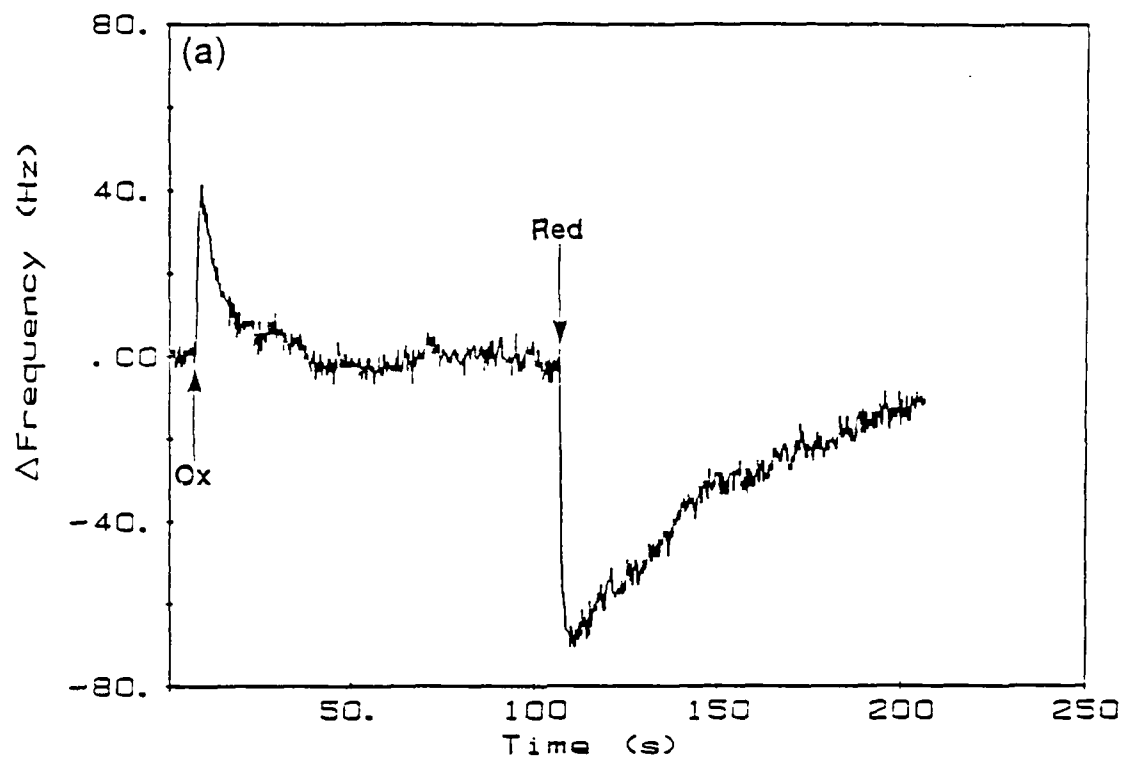
E (volts) vs. Ag/Ag<sup>+</sup> (0.1M)

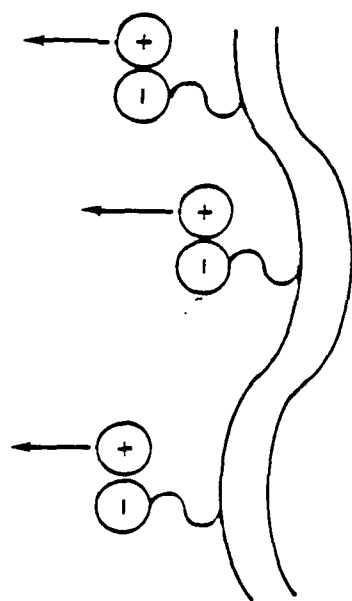
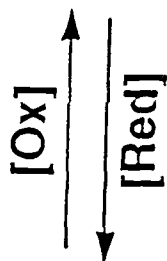
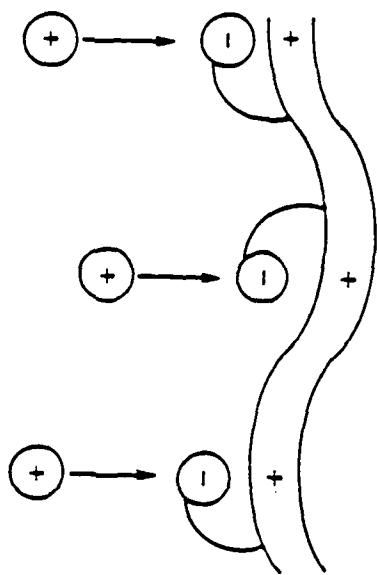












# Scheme I

